Ancestral SARS-CoV-2 immune imprinting persists on RBD but not NTD after sequential Omicron infections

Zuowei Wang[1,2], Ling Li[1,2], Ruiping Du[1], Xixian Chen[1], Yi Sun[1], Rongrong Qin[1], Yunjian Li[1], Hualong Feng[1], Lin Hu[1], Xuanyi Chen[1], Maosheng Lu[1], Liwei Jiang[1,*], Teng Zuo[1,*]

[1]Laboratory of Immunoengineering, Institute of Health and Medical Technology, Hefei Institutes of Physical Science, Chinese Academy of Sciences, Hefei 230031, China

[2]These authors contributed equally to this work

*Correspondence: jlw0531@cmpt.ac.cn (L.J.); zuot@cmpt.ac.cn (T.Z.)

Abstract

Whether Omicron exposures could overcome ancestral SARS-CoV-2 immune imprinting remains controversial. Here we analyzed B cell responses evoked by sequential Omicron infections in vaccinated and unvaccinated individuals. Plasma neutralizing antibody titers against ancestral SARS-CoV-2 and variants indicate that immune imprinting is not consistently induced by inactivated or recombinant protein vaccines. However, once induced, immune imprinting is not countered by successive Omicron challenges. We compared binding specificities, neutralizing capacities, developing origins and targeting epitopes of monoclonal antibodies from individuals with or without immune imprinting. Although receptor-binding domain (RBD) and N-terminal domain (NTD) of spike are both primary targets for neutralizing antibodies, immune imprinting only shapes antibody responses to RBD by impeding the production of Omicron-specific neutralizing antibodies while facilitating the development of broadly neutralizing antibodies. We propose that immune imprinting can be either neglected by NTD-based vaccines to induce variant-specific antibodies or leveraged by RBD-based vaccines to induce broadly neutralizing antibodies.

31 **Introduction**

32 Immunological memory is a hallmark of adaptive immunity, which consists of humoral
33 and cellular immunity(1). Upon primary exposure to an antigen, humoral immune
34 responses typically start from priming of naive B cells through cognate interaction
35 between B cell receptor (BCR) and antigen in follicles of secondary lymphoid organs(2).
36 Primed B cells migrate to the border between B cell follicle and T cell zone, where they
37 encounter activated CD4 T cells. Cognate T-B interaction leads to clonal expansion of
38 B cells and formation of germinal centers (GCs). Within GCs, B cells undergo somatic
39 hypermutation (SHM) on variable region of BCR to generate a pool of mutated B cells,
40 which are then selected based on their affinities to the antigen. After repeated rounds
41 of mutation and selection, affinity-matured GC B cells differentiate into plasmablasts
42 (PBs), plasma cells (PCs) or memory B cells. PB/PCs constantly secrete antibodies
43 and maintain high levels of serum antibodies for months to years. Meanwhile, memory
44 B cells circulate throughout the body until they encounter cognate antigens. Activated
45 memory B cells rapidly differentiate into PB/PCs to secrete antibodies, or to a lesser
46 extent, into GC B cells to undergo another round of affinity maturation(3).

47 As the basic principle of long-term immune protection against pathogens after infection
48 or vaccination, immunological memory ensures much faster and stronger immune
49 responses upon antigen re-exposure(1). However, the effects of immunological
50 memory could be undesirable when antigens in prior and subsequent exposures are
51 heterologous but antigenically related. One example of such scenario is that
52 individuals' antibody responses against influenza viruses are largely biased towards

53 the predominant strains in their early lives(4). This phenomenon is referred to as
54 original antigenic sin or immune imprinting, which describes the effects of immunity
55 elicited by prior antigen exposures on subsequent immune responses to antigenically
56 related antigens.
57 Since the outbreak of COVID-19 pandemic, the ancestral SARS-CoV-2 has kept
58 evolving and generated hundreds of thousands of variants. Among them, Omicron
59 emerged in November 2021 and accumulated more than 30 mutations on spike, the
60 target of neutralizing antibodies(5). Over the past two and a half years, the
61 predominant strains have been rapidly iterated by Omicron-derived variants, including
62 BA.1, BA.2, BA.4, BA.5, BQ.1, XBB.1.5, XBB.1.16, XBB.1.9, EG.5.1 and BA.2.86.
63 These variants exhibit unprecedented neutralization evasion from antibodies elicited
64 by ancestral SARS-CoV-2 infection or vaccines based on ancestral SARS-CoV-2 (6-
65 11). Consequently, several waves of infection by Omicron variants have occurred and
66 updated vaccines have been developed to match those variants (12-14).
67 Analysis of B cell responses in individuals who experienced breakthrough infection of
68 Omicron variants or received Omicron booster vaccines demonstrates the induction of
69 immune imprinting by ancestral SARS-CoV-2(15-20). Moreover, the imprinted antibody
70 responses display substantially reduced neutralizing activities against later Omicron
71 variants compared with ancestral SARS-CoV-2 and earlier Omicron variants,
72 highlighting that immune imprinting may impede the generation of neutralizing
73 antibodies against future SARS-CoV-2 variants or other related viruses(21). Notably,
74 a recent study reported that sequential Omicron exposures could overcome immune

75 imprinting and induce a large portion of *de novo* Omicron-specific antibodies(22). In
76 contrast, other studies concluded that a single exposure to antigenically distant
77 XBB.1.5 or double exposures to Omicron variants rarely elicited Omicron-specific
78 antibody responses in the presence of immune imprinting(23-25). Therefore, it is
79 controversial whether Omicron exposures could override ancestral SARS-CoV-2
80 immune imprinting.

81 In this study, we compared human B cell responses elicited by sequential Omicron
82 infections in the presence or absence of ancestral SARS-CoV-2 immune imprinting.
83 By measuring plasma neutralizing antibody titers against ancestral SARS-CoV-2 and
84 variants, we find that immune imprinting is not consistently induced by inactivated or
85 recombinant protein vaccines. However, once induced, immune imprinting is not
86 countered by repeated Omicron exposures. Comprehensive analysis of monoclonal
87 antibodies from individuals with or without immune imprinting demonstrates that RBD
88 and NTD are both primary targets for neutralizing antibodies, whereas only RBD-
89 specific antibody responses are imprinted. Consequently, Omicron-specific
90 neutralizing antibodies to RBD are hindered while broadly neutralizing antibodies to
91 RBD are elicited. These findings provide new insights into the development of next-
92 generation SARS-CoV-2 vaccines.

93 **Results**

94 **Sequential Omicron infections could not overcome ancestral SARS-CoV-2**
95 **immune imprinting induced by inactivated or recombinant RBD vaccines.**

96 To examine whether Omicron exposures could overcome ancestral SARS-CoV-2
97 immune imprinting, we collected peripheral blood from 12 donors of sequential
98 Omicron infections (Figure 1A). They were first infected in December 2022 or January
99 2023, when BA.5 and BF.7 were predominant strains(26). Around half a year later,
100 they were infected again when XBB lineages (XBB*) were predominant strains(27).
101 Before the infections, Donor A and B were not administrated with any vaccines based
102 on ancestral SARS-CoV-2, while the other donors received two or three doses of
103 inactivated vaccine or recombinant RBD vaccine or in combination.
104 We measured plasma neutralizing antibody titers against a panel of 18 pseudoviruses
105 bearing spikes from ancestral SARS-CoV-2 (WT), Alpha, Beta, Gamma, Delta, BA.1,
106 BA.4/5, BA.2.75, XBB, XBB.1.5, EG.5, EG.5.1, FL.1.5, FL.1.5.1, HK.3, BA.2.86, JN.1
107 and SARS-CoV-1 (Figure S1A). Donor A-D show poor or lower neutralizing titers
108 against earlier SARS-CoV-2 strains from WT to BA.1 while higher titers against strains
109 from BA.4/5 to HK.3 (Figure 1B). As Donor A and B were unvaccinated, their patterns
110 represent antibody responses induced by sequential Omicron exposures in the
111 absence of immune imprinting. Despite the fact that Donor C and D were vaccinated,
112 they display similar patterns with Donor A and B, suggesting that immune imprinting is
113 not induced by vaccination in Donor C and D. Donor E-K maintain higher titers against
114 earlier strains from WT to BA.2.75 while lower titers against XBB and later strains,
115 indicating the presence of immune imprinting in these individuals (Figure 1C). Different
116 from above donors, Donor L exhibits a quite chaotic pattern of neutralizing titers and
117 thus is excluded for further analysis (Figure S1B).

118 We compared neutralizing titers of Donor A-D (referred to as unimprinted group, G1)
119 and Donor E-K (referred to as imprinted group, G2) (Figure 1D). For early strains from
120 WT to BA.1, imprinted group has significantly higher titers than unimprinted group. On
121 the contrary, for more recent Omicron variants, including XBB, XBB.1.5, EG.5, EG.5.1,
122 FL.1.5 and HK.3, unimprinted group surpasses the imprinted group. Taken together,
123 these data suggest that immune imprinting is not consistently induced by vaccination.
124 However, once induced, immune imprinting is not countered by sequential Omicron
125 infections.

126 **Immune imprinting leads to more frequent cross-reactive antibodies to RBD but**
127 **not NTD**

128 To decipher the effects of immune imprinting on human B cell responses elicited by
129 sequential Omicron infections, we moved on to isolate and characterize monoclonal
130 antibodies (mAbs) from those donors. As they were sequentially exposed to BA.5/BF.7
131 and XBB*, we sorted single memory B cells or plasmablasts with XBB.1.5 spike as bait
132 (Figure S2). After cloning antibody variable regions from single cells into corresponding
133 antibody-expressing vectors, we transfected HEK293T cells with paired plasmids and
134 collected supernatant for ELISA and neutralization assay. The supernatant was tested
135 against spike (S), S1, RBD, NTD and S2 of XBB.1.5 and WT by ELISA, and tested
136 against XBB.1.5 and WT pseudoviruses by neutralization assay (Figure 2A). In total,
137 we identified 364 clones positive for XBB.1.5 spike from Donor A, B, C, D, E, F, G, I, J
138 and K. The proportions of antibodies against each domain vary in a wide range and no
139 significant differences are observed between unimprinted group (G1) and imprinted

140 group (G2) (Figure 2B). With 50% as cutoff for neutralization of supernatant, 84 clones
141 were identified as neutralizing antibodies against XBB.1.5 or WT or both (Figure 2A,
142 B). Notably, cross-neutralizing antibodies are all from imprinted group (Figure 2A). In
143 addition, the vast majority of neutralizing antibodies target either RBD or NTD and
144 there are no significant differences between the two groups (Figure 2B).
145 We further analyzed the frequency of cross-reactive antibodies (XBB.1.5^{+} WT^{+}) (Figure
146 2C, D). Most S2-specific antibodies are cross-reactive, which should be due to the
147 conservation of this domain. For NTD-specific antibodies, the frequencies range from
148 0 to 50% and there is no difference between G1 and G2. In contrast, for RBD-specific
149 antibodies, G2 has remarkably higher frequency than G1, which represents recall of
150 cross-reactive memory B cells induced by vaccination. Overall, these results indicate
151 that immune imprinting mainly influences antibody responses to RBD after sequential
152 Omicron infections.

153 **Immune imprinting facilitates the development of broadly neutralizing**
154 **antibodies against RBD**

155 To determine the effects of immune imprinting on neutralizing antibodies, we purified
156 RBD- or NTD-specific mAbs with supernatant neutralization above or close to 50%. A
157 total number of 87 mAbs, including 16 RBD-specific and 32 NTD-specific mAbs from
158 G1 and 33 RBD-specific and 6 NTD-specific mAbs from G2, were tested against a
159 panel of SARS-CoV-2 pseudoviruses (Figure 3A). Similar to the neutralization patterns
160 of plasma from G1, RBD-specific mAbs from G1 (G1-RBD) poorly neutralize early
161 strains from WT to BA.1 while potently neutralize later Omicron variants. RBD-specific

162 mAbs from G2 can be divided into two subgroups according to their neutralization
163 patterns. One subgroup resembles mAbs from G1-RBD in neutralization pattern and
164 is named as non-WT-neutralizing (Abbreviated as non-WT-neut). The other subgroup
165 replicates the neutralization patterns of plasma from G2 and is termed as WT-
166 neutralizing (Abbreviated as WT-neut). It is worth mentioning that there are several
167 broadly neutralizing antibodies in this group, including KXD-E1, KXD-F3, KXD-F1,
168 KXD-G10 and KXD-G5. Most NTD-specific mAbs are able to neutralize BA.4/5, BQ.1,
169 XBB, XBB.1.5, EG.5.1 and HK.3, and the patterns are similar between G1 and G2.
170 Regarding to the neutralizing potency (IC50s) against different strains, mAbs from G1-
171 RBD are more potent to BA.4/5 than later variants whereas mAbs from G2-RBD-non-
172 WT-neut exhibit similar neutralizing activity against BA.4/5 and later strains (Figure
173 S3A). Antibodies from G2-RBD-WT-neut have equivalent potency to early strains from
174 WT to BA.4/5 while decreased potency to later variants (Figure S3A). Different from
175 RBD-specific mAbs, NTD-specific mAbs from both G1 and G2 are most potent to XBB
176 and XBB.1.5 (Figure S3B).
177 We compared the neutralizing potency of mAbs from different groups against the same
178 strain (Figure 3B,3C). Overall, mAbs from G1-RBD have similar neutralizing potency
179 with mAbs from G2-RBD-non-WT-neut. However, mAbs from G1-RBD are more potent
180 than mAbs from G2-RBD-WT-neut against variants from BA.4/5 to JN.1 except
181 BA.2.75 and XBB. On the other hand, NTD-specific mAbs from both groups have
182 analogous potency against all tested strains except HK.3. These data further confirm
183 that antibody responses to RBD while not NTD are affected by immune imprinting.

184 Moreover, the imprinted RBD-specific antibodies tend to have broadly neutralizing
185 activity although they generally show suboptimal neutralizing potency against Omicron
186 variants.

187 **Repeated Omicron infections induce de novo Omicron-specific antibody**
188 **responses in the presence of immune imprinting**

189 To examine whether repeated Omicron infections could induce de novo antibody
190 responses from naïve B cells in the presence of immune imprinting, we move on to
191 investigate the origins of neutralizing mAbs from each group. In published literatures,
192 it is generally assumed that cross-reactive antibodies derive from memory B cells
193 induced by WT whereas omicron-specific antibodies originate from naïve B cells
194 activated by Omicron(22-25). However, these assumptions remain to be confirmed by
195 experiments to exclude possibilities that memory B cells induced by WT may lose
196 cross-reactivity and Omicron-specific naïve B cells may develop cross-reactivity during
197 affinity maturation. Here, we constructed germline versions of representative mAbs
198 from each group and tested their binding to a panel of spikes expressed on HEK293T
199 cells by FACS (Figure 4A). Germline antibodies from G1-RBD, G2-RBD-non-WT-neut,
200 G1-NTD and G2-NTD bind Omicron spikes but not WT spike. Oppositely, germline
201 antibodies from G2-RBD-WT-neut mostly recognize WT spike but not Omicron spikes.
202 These data confirm that mAbs from G1-RBD, G2-RBD-non-WT-neut, G1-NTD and G2-
203 NTD are de novo antibodies induced by Omicron, whereas mAbs from G2-RBD-WT-
204 neut are recalled antibodies initially induced by WT.

205 Correlated with their origins, mAbs from G2-RBD-WT-neut show higher mutation levels
206 than other mAbs, which reflects extensive affinity maturation sequentially driven by WT
207 and Omicron (Figure 4B). On the other hand, we also analyzed the repertoire of each
208 group (Figure 4C and Table 1). In G2-RBD-WT-neut group, IGHV1-18 and IGLV1-44
209 are most frequent as a consequence of B cell clonal expansion in Donor J. Moreover,
210 IGHV3-53, IGHV3-66 and IGHV1-69, which have been identified as frequent VH genes
211 for RBD-specific antibodies from individuals exposed to WT spike(28, 29), are
212 frequently used in G2-RBD-WT-neut but not in G1-RBD and G2-RBD-non-WT-neut.
213 For NTD-specific antibodies, IGHV4-39 is most frequently used and is identified from
214 multiple donors in both groups. Therefore, these IGHV4-39 antibodies can be taken as
215 a class of public antibody against NTD. In sum, these data suggest that repeated
216 Omicron exposures could induce de novo antibody responses to RBD and NTD in the
217 presence of immune imprinting.

218 **Omicron-specific and WT-cross-reactive antibodies recognize similar epitopes**

219 To determine whether de novo antibody responses induced by repeated Omicron
220 infections recognize distinct epitopes compared with WT-cross-reactive antibodies, we
221 performed competition ELISA (Figure 5A, 5B). Three broadly neutralizing antibodies
222 targeting RBD, including BD55-1205, BD56-1854 and BD55-5483 were taken as
223 reference(30). A major cluster is formed by the majority of RBD-specific antibodies.
224 Most antibodies in this cluster also compete with BD55-1205, BD56-1854 and ACE2.
225 Outside the major cluster, a minor cluster is formed by 6 antibodies. They compete
226 with BD55-5483 but not with BD55-1205, BD56-1854 and ACE2. The rest 3 RBD-

227 specific antibodies do not exhibit apparent competition with other antibodies or ACE2.
228 On the other hand, NTD-specific antibodies show competition with each other and form
229 a single cluster, suggesting that NTD-specific neutralizing antibodies target a supersite.
230 Taken together, these data provide explanation for the suppressed Omicron-specific
231 antibody responses to RBD in the presence of immune imprinting.

232 **Discussion**

233 In this study, we compared B cell responses evoked by sequential Omicron infections
234 in individuals vaccinated or unvaccinated with inactivated or recombinant RBD
235 vaccines. Unexpectedly, two vaccinees show no hints of immune imprinting, according
236 to their polyclonal and monoclonal antibody responses against ancestral SARS-CoV-
237 2 and variants. Therefore, they are classified into unimprinted group along with two
238 unvaccinated individuals throughout this study. Considering the factor of individual
239 variations, we believe that this classification is more reasonable than simply grouping
240 the cohorts based on antigen exposure history, especially for cohorts with limited size.
241 We speculate that no immune imprinting in these two individuals is probably due to
242 weak immune responses stimulated by vaccination. Moreover, whether this
243 phenomenon is common remains to be determined with larger cohorts.

244 In contrast to individuals without immune imprinting, individuals with immune imprinting
245 have lower plasma neutralizing antibody titers against multiple Omicron variants after
246 XBB, along with more frequent WT-cross-reactive antibodies and less frequent
247 Omicron-specific antibodies to RBD. Therefore, we conclude that immune imprinting
248 induced by inactivated or recombinant RBD vaccines is not countered by sequential

249 Omicron infections, which is inconsistent to a study performed by Yisimayi et al(22).
250 We suppose this contradiction is due to following factors. First, the infections were
251 sequentially caused by BA.1/BA.2 and BA.5/BF.7 in their study whereas by BA.5/BF.7
252 and XBB* in our study. We notice that individuals with or without immune imprinting
253 have equivalent plasma neutralizing antibody titers to BA.4/5 and BA.2.75. Moreover,
254 individuals with immune imprinting show unaffected neutralizing titers against early
255 Omicron variants including BA.1, BA.2.75 and BA.4/5 compared with WT. These data
256 suggest that immune imprinting does not compromise antibody responses to early
257 Omicron variants after repeated Omicron exposures. Second, all vaccinees were
258 considered as imprinted in their study while two vaccinees were taken as unimprinted
259 in our study. As vaccinees without immune imprinting are able to generate abundant
260 Omicron-specific antibodies, excluding them from imprinted cohort may lead to more
261 clear results.
262 A major finding of our study is that antibody responses to NTD are not affected by
263 immune imprinting. As immunological memory and cross-reactivity are the basis of
264 immune imprinting(31), one possible explanation for this finding is that NTD is less
265 immunogenic than RBD because of its extensive glycan shielding(32, 33), and thus
266 few NTD-specific memory B cells are induced. Another possible explanation is that
267 NTD-specific memory B cells induced by WT are not cross-reactive to Omicron
268 variants. However, consistent with previous studies(34-39), our results argue that NTD
269 is highly immunogenic and able to elicit antibodies cross-reactive to XBB.1.5 and WT,
270 which meet the preconditions for immune imprinting. Therefore, the mechanisms for

271 the unimprinted antibody responses to NTD remain to be explored.

272 Similar to previous studies(15-18, 20, 22-24), we prove that immune imprinting
273 persistently shapes antibody responses to RBD. As a result, RBD-specific antibodies
274 can be divided into two groups: WT-cross-reactive antibodies and Omicron-specific
275 antibodies. Compared with Omicron-specific antibodies, WT-cross-reactive antibodies
276 tend to have broader neutralization spectrum. For example, KXD-F1 neutralize all
277 tested pseudoviruses from WT to JN.1 with IC50s ranging from 0.006 to 0.084 μg/ml.
278 As germlines of those WT-cross-reactive antibodies generally have limited breadth,
279 there is no doubt that the breadth of WT-cross-reactive antibodies is attributed to
280 affinity maturation. However, the underlying mechanisms are not fully understood.
281 According to the model of affinity maturation in GCs, it is possible that WT-cross-
282 reactive memory B cells become Omicron-specific after affinity maturation. By
283 comparing the binding specificities of paired germline and mature antibodies, we find
284 that all WT-reactive germline antibodies consistently recognize WT spike after affinity
285 maturation, which negate the possibility like our previous study(40). Oppositely, it is
286 also possible that Omicron-specific naïve B cells may become cross-reactive after
287 affinity maturation. However, we have not found evidence to support the possibility,
288 despite that fact that infection or vaccination with WT could elicit broadly neutralizing
289 antibodies against Omicron variants(30, 41-43). More studies are required to solve
290 these puzzles on affinity maturation.

291 Currently, ancestral SARS-CoV-2 immune imprinting has been acknowledged as a
292 great barrier for vaccine update. According to our findings, we propose that NTD-based

293 vaccines could be designed to bypass immune imprinting, since NTD is also a major
294 target of neutralizing antibodies. On the other hand, vaccines containing RBD could
295 be designed to leverage the potential of immune imprinting in eliciting broadly
296 neutralizing antibodies.

297 **Materials and methods**

298 **Ethics statement**

299 This study was approved by the Ethics Committee of Hefei Institutes of Physical
300 Science, Chinese Academy of Sciences (Approval Number: YXLL-2023-47). All donors
301 provided written informed consent for collection of information, analysis of plasma and
302 PBMCs, and publication of data generated from their samples.

303 **Human samples**

304 Peripheral blood samples were collected from 12 donors (Figure1A). Plasma and
305 peripheral blood mononuclear cells (PBMCs) were separated from blood by Ficoll
306 density gradient centrifugation.

307 **Cell lines**

308 HEK293T cells expressing human ACE2 (HEK293T-hACE2) were kindly provided by
309 Prof. Ji Wang at Sun Yat-Sen University. HEK293T cells were from ATCC. HEK293T
310 and HEK293T-hACE2 cells were cultured in DMEM with 10% fetal bovine serum (FBS,
311 VivaCell, Shanghai, China, C04001) and 1% penicillin/streptomycin (pen/strep).
312 FreeStyle 293F cells (Thermo Fisher Scientific) were cultured in SMM 293-TII
313 Expression Medium (Sino Biological Inc., M293TII). All cells were maintained in a 37˚C
314 incubator at 5% CO_2

315 **Protein expression and purification**

316 The genes encoding the ectodomain of SARS-CoV-2 spike including WT and XBB.1.5
317 were constructed with foldon trimerization motif, His tag, tandem strep-tag II and FLAG
318 tag at C-terminal. The genes encoding the S1, NTD and RBD of WT and XBB.1.5 were
319 constructed with a strep-tag II at C-terminal. The genes encoding the S2 of WT and
320 XBB.1.5 were constructed with a His tag at C-terminal. Spike trimer, S1, S2, NTD and
321 RBD were expressed in the FreeStyle 293F cells and purified by Streptactin Agarose
322 Resin 4FF (Yeasen, 20495ES60) or Ni-NTA Agarose (Qiagen, 30210).

323 **Spike-specific Single B cell sorting and PCR**

324 PBMCs were incubated with 200nM XBB.1.5 spike for 30 min at 4˚C. After wash, they
325 were stained with cell-surface antibodies: CD3-BV510 (BioLegend, 317331), CD19-
326 PE/Cy7 (BioLegend, 302215), CD27-APC (BioLegend, 356409), CD38-APC/Cy7
327 (BioLegend, 356615), human IgM-AF700 (BioLegend, 314537), human IgD-
328 perCP/Cy5.5 (BioLegend, 348207), anti-His-AF488 (Proteintech, CL488-66005), anti-
329 FLAG-PE (BioLegend, 637309) and DAPI. The stained cells were washed with FACS
330 buffer (PBS containing 2% FBS) and resuspended in 500μl FACS buffer. Spike-specific
331 single B cells were gated as $DAPI^{-}CD3^{-}CD19^{+}CD27^{+}IgD^{-}His^{+}FLAG^{+}$ and sorted into
332 96-well PCR plates containing 4μl lysis buffer (0.5×PBS, 0.1M DTT and RNase
333 inhibitor) per well. After reverse transcription reaction, variable regions of heavy and
334 light chains were amplified by nested PCR and cloned into human IgG1 expression
335 vectors. Plasmids for paired heavy and light chains were co-transfected into HEK293T
336 cells or FreeStyle 293F cells. Antibodies were purified with Protein A magnetic beads

337 (GenScript, L00273).

338 **ELISA**

339 Spike, S1, S2, NTD or RBD were coated onto 96-well ELISA plates (100 ng/well) and
340 incubated at 4˚C overnight. After blocking with PBS containing 10% FBS, HEK293T
341 supernatant was added to the wells and incubated at 37˚C for 1hr. HRP-conjugated
342 goat anti-human IgG antibodies (Zen-bio, 550004; 1:2000 dilution) were added to the
343 wells and incubated at 37˚C for 1hr. TMB substrate (Sangon Biotech, E661007-0100)
344 was added to the wells and incubated at room temperature for 5 mins. The reaction
345 was stopped by TMB Stop Solution (Sangon Biotech, E661006-0500) and absorbance
346 at 450 nm was measured.

347 **Pseudovirus neutralization assay**

348 To generate pseudoviruses, HEK293T cells were transfected with psPAX2, pLenti-
349 luciferase and spike-encoding plasmids using polyetherimide (PEI). Supernatants with
350 pseudoviruses were collected 48hrs after transfection. 3-fold serially diluted plasma
351 (starting at 1:20), HEK293T supernatant (starting at 1:4.5), or mAbs (starting at
352 10μg/ml) were mixed with pseudoviruses at 37˚C for 1hr. HEK293T-hACE2 cells
353 (1.5×10^4 per well) were added into the mixture and incubated at 37˚C for 48hrs. Cells
354 were lysed to measure luciferase activity by Bright-Lite Luciferase Assay System
355 (Vazyme Biotech, DD1204-02). The percentages of neutralization were determined by
356 comparing with the virus control. The plasmids encoding spike of WT, Alpha, Beta,
357 Gamma, Delta, BA.1, BA.4/5, XBB, XBB.1.5 and SARS-CoV-1 were kindly provided
358 by Prof. Linqi Zhang at Tsinghua University. The plasmids encoding spike of BA.2.75

359 was kindly provided by Prof. Zezhong Liu at Fudan University. The sequences of EG.5,
360 EG.5.1, FL.1.5, FL.1.5.1, HK.3, BA.2.86 and JN.1 spike were synthesized and cloned
361 into expression vectors.

362 **Competition ELISA**

363 NTD-specific and RBD-specific neutralizing mAbs were labeled with HRP (ProteinTech,
364 PK20001). XBB.1.5 spike was coated onto 96-well ELISA plates (50 ng/well) and
365 incubated at 4˚C overnight. After blocking with PBS containing 10% FBS, blocking
366 mAbs were added to the wells and incubated at 37˚C for 1hr. HRP-labeled detecting
367 mAbs were added to the wells in the presence of competing mAbs. The ratio of
368 blocking antibody and detecting antibody is 100:1. After 1hr incubation at 37˚C, TMB
369 substrate (Sangon Biotech, E661007-0100) was added to the wells and incubated at
370 room temperature for 30 mins. The reaction was stopped by TMB Stop Solution
371 (Sangon Biotech, E661006-0500) and absorbance at 450 nm were measured. The
372 percentages of signal decrease caused by blocking mAbs were calculated.

373 **ACE2 competition FACS**

374 5nM biotinylated XBB.1.5 spike was incubated with 10μg/ml competing mAbs for
375 30min at 4˚C, then the mixtures were added to HEK293T-hACE2 cells. After 30min at
376 4˚C, the cells were washed with FACS buffer. Streptavidin-APC (BioLegend, 405207)
377 and DAPI were added to the wells at 4˚C for 30min. The stained cells were washed
378 with FACS buffer and resuspended in 200μl FACS buffer. Positive cells were gated as
379 $DAPI^{-}$XBB.1.5 $spike^{+}$. The percentages of signal decrease caused by competing mAbs
380 were calculated.

381 **Germline antibodies binding FACS**

382 The plasmids encoding spikes of SARS-CoV-2 WT, Alpha, Beta, Gamma, Delta, BA.1,
383 BA.4/5, BF.7, BA.2.75, BQ.1, XBB.1.5, EG.5.1, BA.2.86 were transfected into
384 HEK293T cells. After 48hr, cells were harvested and incubated with 50μg/ml germline
385 antibodies for 30min at 4˚C. After washed with FACS buffer, cells were stained with
386 goat anti-human IgG FITC (Proteintech, SA00003-12) and DAPI. The stained cells
387 were washed with FACS buffer and resuspended in 200μl FACS buffer. Positive cells
388 were gated as $DAPI^{-}IgG^{+}$.

389 **Acknowledgements**

390 The authors thank all donors for providing peripheral blood. This work was supported
391 by the National Key Plan for Scientific Research and Development of China (Grant No.
392 2022YFC2305800) and the National Natural Science Foundation of China (Grant No.
393 32200765, Grant No. 32370941).

394 **References**

395 1. D. Gray, Immunological memory. *Annu Rev Immunol* **11**, 49-77 (1993).
396 2. G. D. Victora, M. C. Nussenzweig, Germinal Centers. *Annu Rev Immunol* **40**, 413-442
397 (2022).
398 3. L. Mesin *et al.*, Restricted Clonality and Limited Germinal Center Reentry Characterize
399 Memory B Cell Reactivation by Boosting. *Cell* **180**, 92-106 e111 (2020).
400 4. T. Francis, On the Doctrine of Original Antigenic Sin. *Proceedings of the American*
401 *Philosophical Society* **104**, 572-578 (1960).
402 5. R. Viana *et al.*, Rapid epidemic expansion of the SARS-CoV-2 Omicron variant in southern
403 Africa. *Nature* **603**, 679-686 (2022).
404 6. Q. He *et al.*, An updated atlas of antibody evasion by SARS-CoV-2 Omicron sub-variants
405 including BQ.1.1 and XBB. *Cell Rep Med* **4**, 100991 (2023).
406 7. C. Kurhade *et al.*, Low neutralization of SARS-CoV-2 Omicron BA.2.75.2, BQ.1.1 and XBB.1
407 by parental mRNA vaccine or a BA.5 bivalent booster. *Nat Med* **29**, 344-347 (2023).
408 8. Q. Wang *et al.*, Alarming antibody evasion properties of rising SARS-CoV-2 BQ and XBB
409 subvariants. *Cell* **186**, 279-286 e278 (2023).
410 9. J. Miller *et al.*, Substantial Neutralization Escape by SARS-CoV-2 Omicron Variants BQ.1.1

411 and XBB.1. *N Engl J Med* **388**, 662-664 (2023).
412 10. Q. Wang *et al.*, Antibody neutralisation of emerging SARS-CoV-2 subvariants: EG.5.1 and
413 XBC.1.6. *Lancet Infect Dis* **23**, e397-e398 (2023).
414 11. S. Yang *et al.*, Fast evolution of SARS-CoV-2 BA.2.86 to JN.1 under heavy immune
415 pressure. *Lancet Infect Dis* **24**, e70-e72 (2024).
416 12. S. Chalkias *et al.*, Safety, immunogenicity and antibody persistence of a bivalent Beta-
417 containing booster vaccine against COVID-19: a phase 2/3 trial. *Nat Med* **28**, 2388-2397
418 (2022).
419 13. S. Chalkias *et al.*, A Bivalent Omicron-Containing Booster Vaccine against Covid-19. *N*
420 *Engl J Med* **387**, 1279-1291 (2022).
421 14. A. Y. Collier *et al.*, Immunogenicity of BA.5 Bivalent mRNA Vaccine Boosters. *N Engl J Med*
422 **388**, 565-567 (2023).
423 15. Y. J. Park *et al.*, Imprinted antibody responses against SARS-CoV-2 Omicron sublineages.
424 *Science* **378**, 619-627 (2022).
425 16. Z. Wang *et al.*, Memory B cell responses to Omicron subvariants after SARS-CoV-2 mRNA
426 breakthrough infection in humans. *J Exp Med* **219** (2022).
427 17. C. I. Kaku *et al.*, Recall of preexisting cross-reactive B cell memory after Omicron BA.1
428 breakthrough infection. *Sci Immunol* **7**, eabq3511 (2022).
429 18. J. Quandt *et al.*, Omicron BA.1 breakthrough infection drives cross-variant neutralization
430 and memory B cell formation against conserved epitopes. *Sci Immunol* **7**, eabq2427
431 (2022).
432 19. T. Weber *et al.*, Enhanced SARS-CoV-2 humoral immunity following breakthrough
433 infection builds upon the preexisting memory B cell pool. *Sci Immunol* **8**, eadk5845 (2023).
434 20. A. Addetia *et al.*, Neutralization, effector function and immune imprinting of Omicron
435 variants. *Nature* **621**, 592-601 (2023).
436 21. Q. Wang *et al.*, Deep immunological imprinting due to the ancestral spike in the current
437 bivalent COVID-19 vaccine. *Cell Rep Med* **4**, 101258 (2023).
438 22. A. Yisimayi *et al.*, Repeated Omicron exposures override ancestral SARS-CoV-2 immune
439 imprinting. *Nature* **625**, 148-156 (2024).
440 23. T. S. Johnston *et al.*, Immunological imprinting shapes the specificity of human antibody
441 responses against SARS-CoV-2 variants. *Immunity* **57**, 912-925 e914 (2024).
442 24. M. A. Tortorici *et al.*, Persistent immune imprinting occurs after vaccination with the
443 COVID-19 XBB.1.5 mRNA booster in humans. *Immunity* **57**, 904-911 e904 (2024).
444 25. C. Y. Liang *et al.*, Imprinting of serum neutralizing antibodies by Wuhan-1 mRNA vaccines.
445 *Nature* 10.1038/s41586-024-07539-1 (2024).
446 26. Y. Pan *et al.*, Characterisation of SARS-CoV-2 variants in Beijing during 2022: an
447 epidemiological and phylogenetic analysis. *Lancet* **401**, 664-672 (2023).
448 27. Y. Feng *et al.*, Genomic Surveillance for SARS-CoV-2 Variants: Dominance of XBB
449 Replacement—China, January–June 2023. *China CDC Weekly* **6**, 324-331 (2024).
450 28. Y. Wang *et al.*, A large-scale systematic survey reveals recurring molecular features of
451 public antibody responses to SARS-CoV-2. *Immunity* **55**, 1105-1117 e1104 (2022).
452 29. Q. Yan *et al.*, Shared IGHV1-69-encoded neutralizing antibodies contribute to the
453 emergence of L452R substitution in SARS-CoV-2 variants. *Emerg Microbes Infect* **11**,
454 2749-2761 (2022).

30. Y. Cao *et al.*, Imprinted SARS-CoV-2 humoral immunity induces convergent Omicron RBD evolution. *Nature* **614**, 521-529 (2023).
31. M. Koutsakos, A. H. Ellebedy, Immunological imprinting: Understanding COVID-19. *Immunity* **56**, 909-913 (2023).
32. A. C. Walls *et al.*, Structure, Function, and Antigenicity of the SARS-CoV-2 Spike Glycoprotein. *Cell* **181**, 281-292 e286 (2020).
33. D. Wrapp *et al.*, Cryo-EM structure of the 2019-nCoV spike in the prefusion conformation. *Science* **367**, 1260-1263 (2020).
34. X. Chi *et al.*, A neutralizing human antibody binds to the N-terminal domain of the Spike protein of SARS-CoV-2. *Science* **369**, 650-655 (2020).
35. L. Liu *et al.*, Potent neutralizing antibodies against multiple epitopes on SARS-CoV-2 spike. *Nature* **584**, 450-456 (2020).
36. M. McCallum *et al.*, N-terminal domain antigenic mapping reveals a site of vulnerability for SARS-CoV-2. *Cell* **184**, 2332-2347 e2316 (2021).
37. N. Suryadevara *et al.*, Neutralizing and protective human monoclonal antibodies recognizing the N-terminal domain of the SARS-CoV-2 spike protein. *Cell* **184**, 2316-2331 e2315 (2021).
38. Z. Wang *et al.*, Analysis of memory B cells identifies conserved neutralizing epitopes on the N-terminal domain of variant SARS-Cov-2 spike proteins. *Immunity* **55**, 998-1012 e1018 (2022).
39. G. Cerutti *et al.*, Neutralizing antibody 5-7 defines a distinct site of vulnerability in SARS-CoV-2 spike N-terminal domain. *Cell Rep* **37**, 109928 (2021).
40. L. Li *et al.*, Breakthrough infection elicits hypermutated IGHV3-53/3-66 public antibodies with broad and potent neutralizing activity against SARS-CoV-2 variants including the emerging EG.5 lineages. *PLoS Pathog* **19**, e1011856 (2023).
41. B. Ju *et al.*, Infection with wild-type SARS-CoV-2 elicits broadly neutralizing and protective antibodies against omicron subvariants. *Nat Immunol* **24**, 690-699 (2023).
42. Y. Liu *et al.*, Inactivated vaccine-elicited potent antibodies can broadly neutralize SARS-CoV-2 circulating variants. *Nat Commun* **14**, 2179 (2023).
43. B. Ju *et al.*, Omicron BQ.1.1 and XBB.1 unprecedentedly escape broadly neutralizing antibodies elicited by prototype vaccination. *Cell Rep* **42**, 112532 (2023).

488 **Figures and tables**

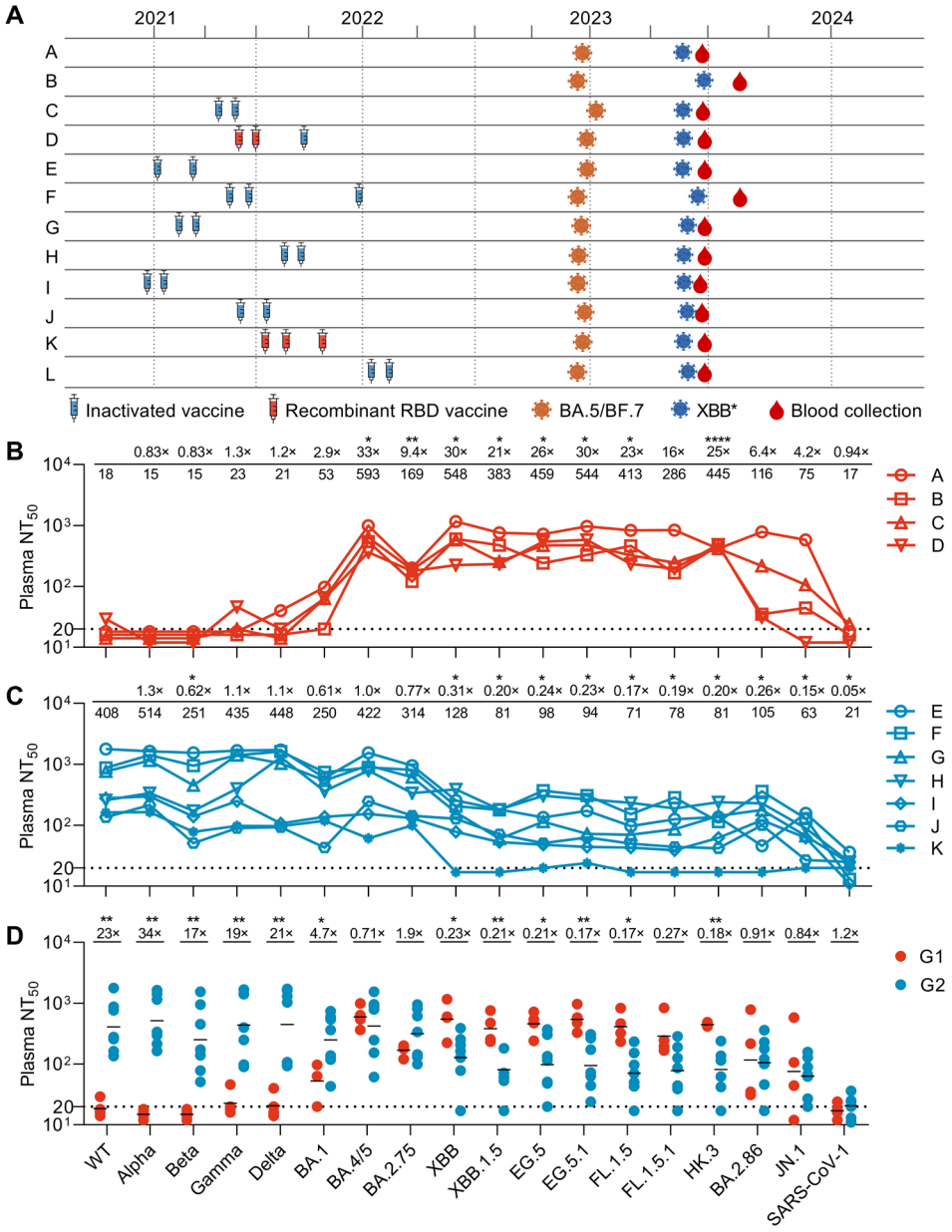

489

490 **Figure 1. Sequential Omicron infections could not overcome ancestral SARS-**

491 **CoV-2 immune imprinting induced by inactivated or recombinant RBD vaccines.**

492 (A) Vaccination and infection information of 12 donors. (B, C) Summary of plasma

493 neutralizing antibody titers (NT50). For plasma with no neutralizing activity at 20-fold

494 dilution, a number between 10–20 is given as titer to separate the curves. The numbers

495 below the line are geometric mean titers against the pseudoviruses. The titers against

496 WT are compared with other variants and the fold changes are indicated above the
497 line. For panel B, statistical analysis was performed by two-tailed paired T test. For
498 panel C, statistical analysis was performed by two-tailed Wilcoxon matched-pairs
499 signed rank test. *P < 0.05, **P < 0.01, **** P < 0.0001. (D) Comparison of neutralizing
500 antibody titers of G1 (Donor A-D, unimprinted group) and G2 (Donor E-K, imprinted
501 group). The numbers on top are fold changes. Statistical analysis was performed by
502 two-tailed unpaired T test. *P < 0.05, **P < 0.01. The neutralizing titers are calculated
503 with results from two independent experiments, in which duplicates are performed.
504

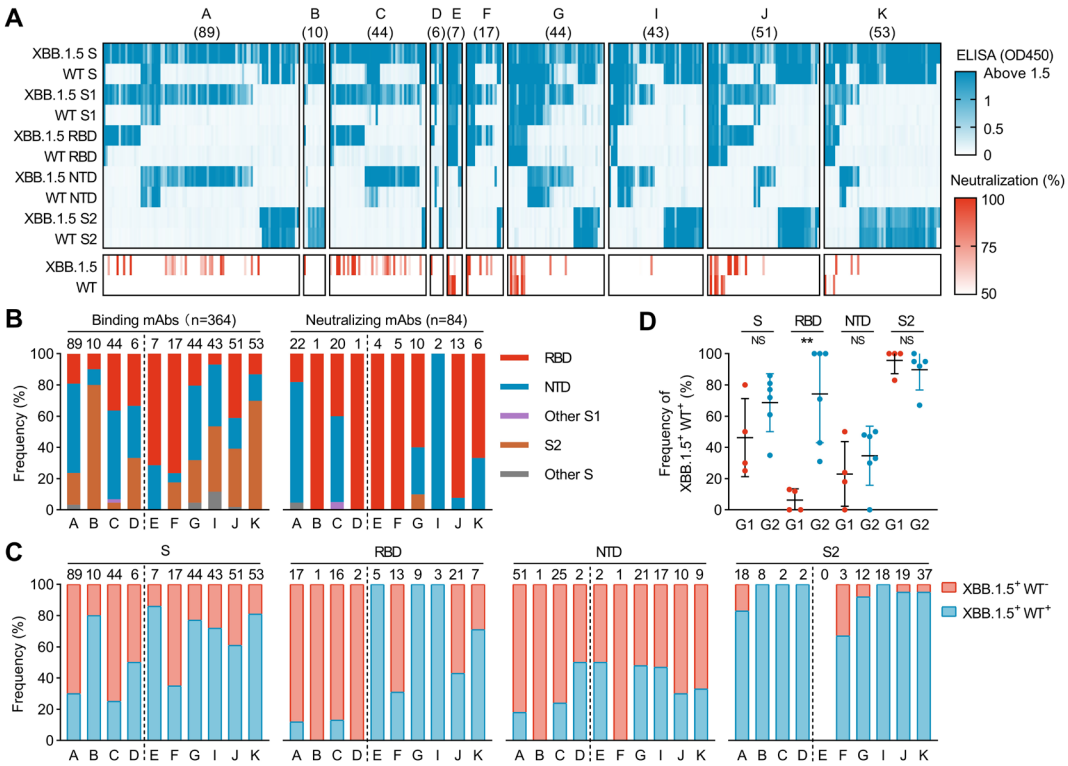

Figure 2. Immune imprinting leads to more frequent cross-reactive antibodies to RBD but not NTD. (A) ELISA and neutralization results of 364 mAbs. Supernatant of HEK293T cells was tested against Spike, S1, S2, NTD and RBD of WT and XBB.1.5 by ELISA, and tested against WT and XBB.1.5. pseudoviruses by neutralization assay. For ELISA, supernatant was not diluted. For neutralization, supernatant was diluted by 4.5-fold. The results are mean values of two independent experiments. For neutralization, duplicates are performed in each experiment. (B) Frequency of binding mAbs and neutralizing mAbs against different domains in each individual. (C) Frequencies of WT-cross-reactive antibodies (XBB.1.5^{+} WT^{+}) and Omicron-specific antibodies (XBB.1.5^{+} WT^{-}) in each individual. (D) Comparison of WT-cross-reactive antibodies between G1 and G2. Data are represented as mean ± SD. Statistical analysis was performed by two-tailed unpaired T test. NS (Not significant) $p > 0.05$, **$P < 0.01$.

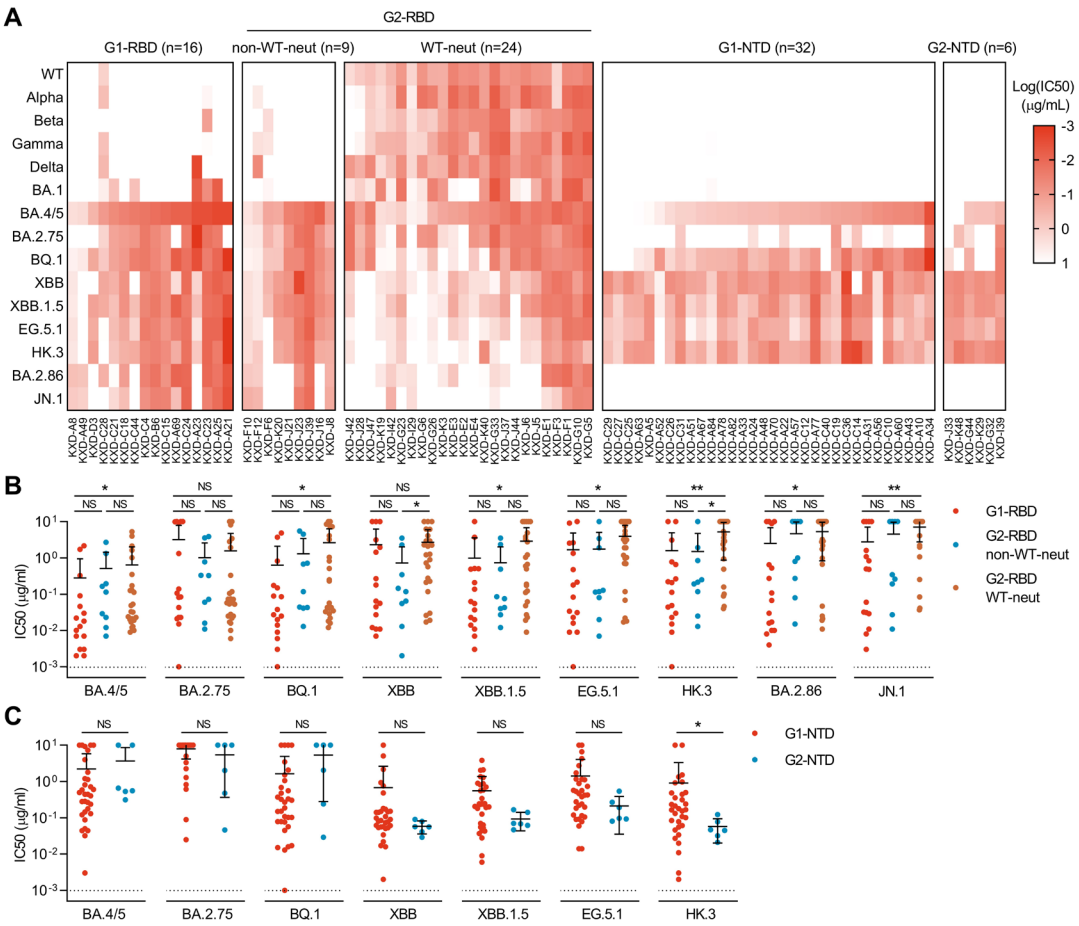

Figure 3. Immune imprinting facilitates the development of broadly neutralizing antibodies against RBD. (A) IC50s of mAbs against WT, Alpha, Beta, Gamma, Delta, BA.1, BA.4/5, BA.2.75, BQ.1, XBB, XBB.1.5, EG.5.1, HK.3, BA.2.86 and JN.1. The highest antibody concentration used to determine IC50 is 10μg/ml. (B) Comparing IC50s of RBD-specific mAbs from three groups. (C) Comparing IC50s of NTD-specific mAbs from two groups. Data are represented as the mean ± SD. Statistical analysis was performed by two-tailed unpaired T test. NS (Not significant) $p > 0.05$, *$P < 0.05$, **$P < 0.01$. IC50s are calculated with results from two independent experiments, in which duplicates are performed.

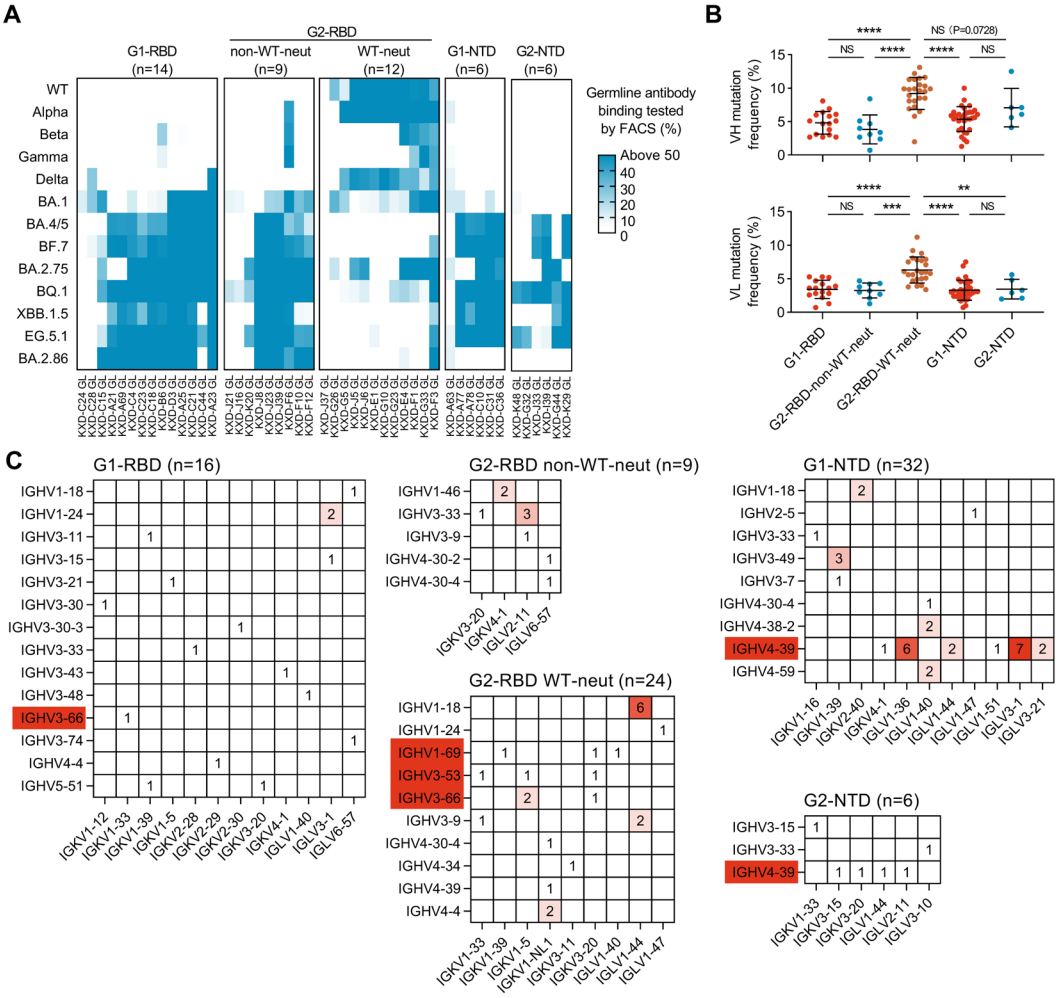

Figure 4. Repeated Omicron infections induce de novo Omicron-specific antibody responses in the presence of immune imprinting. (A) Binding specificities of germline antibodies measured by FACS. HEK293T cells expressing SARS-CoV-2 spikes were incubated with 50μg/ml germline antibodies and analyzed by FACS. The percentages of positive cells are calculated. The results are mean values of two independent experiments. (B) Somatic hypermutations of VH and VL. DNA sequences were analyzed. Data are represented as mean ± SD. Statistical analysis was performed by two-tailed unpaired T test. NS (Not significant) $p > 0.05$, **P < 0.01, ***P < 0.001, ****P < 0.0001. (C) Frequencies of V genes in each group. Frequently used V genes are highlighted by colored background.

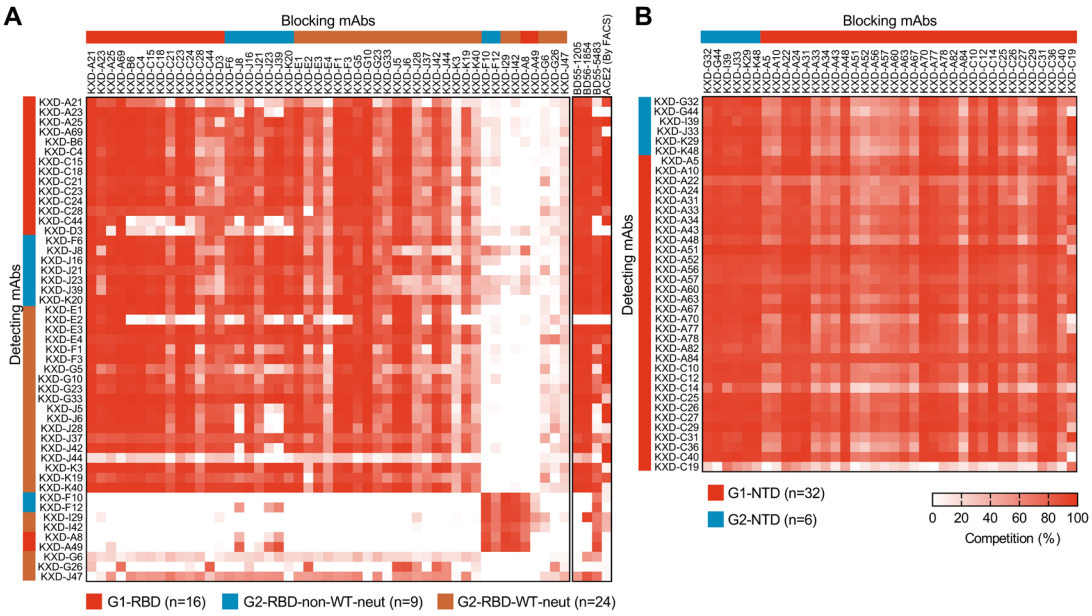

541

542 **Figure 5. Omicron-specific and WT-cross-reactive antibodies recognize similar**

543 **epitopes.** (A) Competition ELISA of RBD-specific mAbs. Competition with ACE2 was

544 performed by FACS. (B) Competition ELISA of NTD-specific mAbs. The results are

545 mean values of two independent experiments.

546

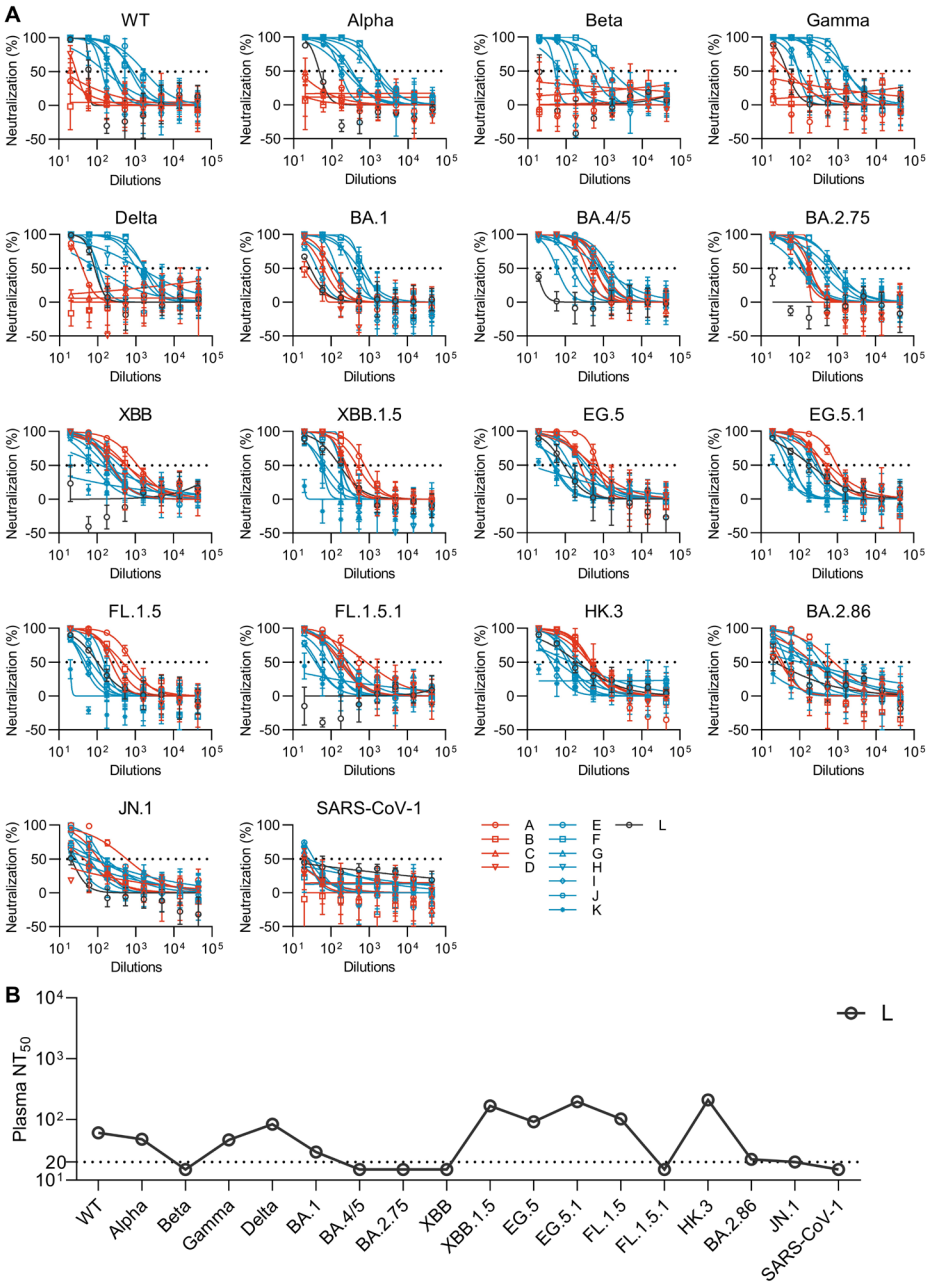

Figure S1. Plasma neutralizing antibody titers. (A) Measurement of neutralizing antibody titers against a panel of pseudoviruses. Data are represented as mean ± SD. (B) Neutralizing antibody titers of donor L.

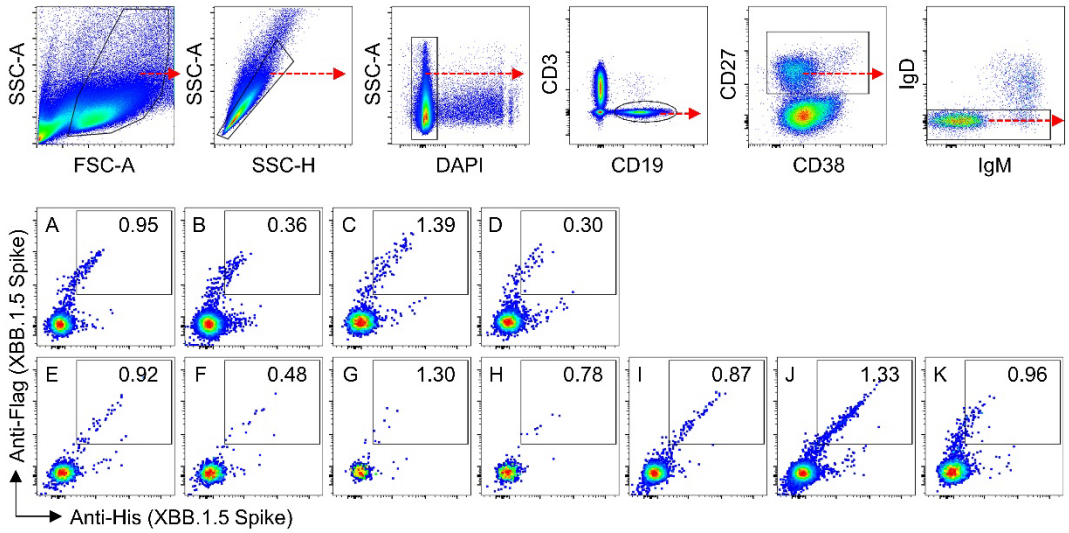

Figure S2. FACS plots representing gating strategies for XBB.1.5 spike-specific single B cell sorting.

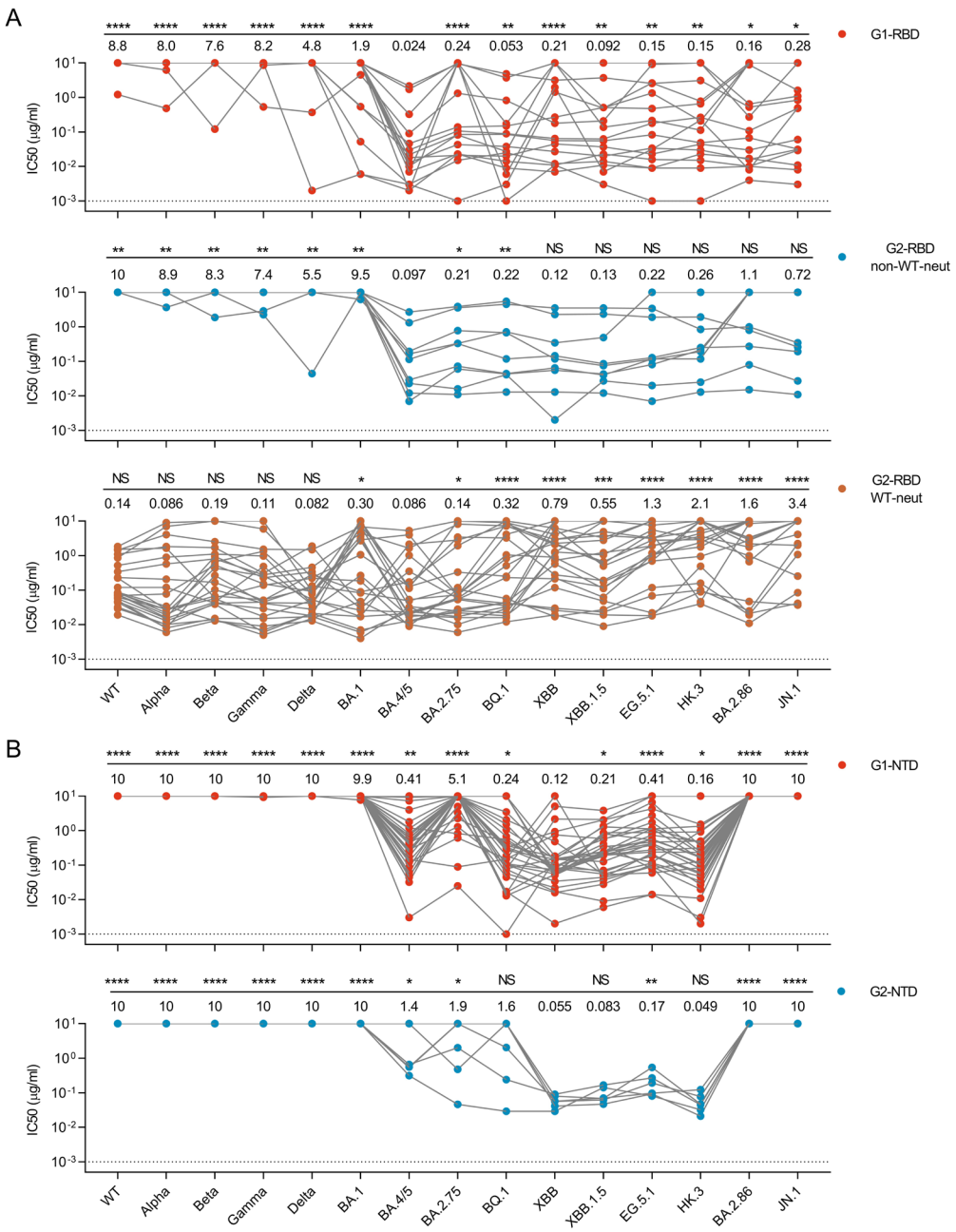

556

557 **Figure S3. Neutralizing potency of mAbs against different variants.** (A) IC50s of

558 RBD-specific mAbs. The numbers below the line are geometric mean IC50 of mAbs

559 against the pseudoviruses. IC50s against BA.4/5 are compared with other variants. (B)

560 IC50s of NTD-specific mAbs. The numbers below the line are geometric mean IC50 of

561 mAbs against the pseudoviruses. IC50s against XBB are compared other variants.

562 Statistical analysis was performed by two-tailed Wilcoxon matched-pairs signed rank

563 test. NS (Not significant) $p > 0.05$, *$P < 0.05$, **$P < 0.01$, ***$P < 0.001$, ****$P < 0.0001$.

564

565 **Table S1. Origins, targets and sequence information of 87 neutralizing mAbs.**

mAbs	Donor	Target	VH						VL				
			V	D	J	CDR3	CDR3 (aa)	SHM(%)	V	J	CDR3	CDR3 (aa)	SHM(%)
KXD-A10	A	NTD	IGHV4-39	IGHD5-12	IGHJ4	ARLRDWDIVAGGGVFDY	17	6.7	IGLV3-1	IGLJ3	QSWDSSTAV	9	2.9
KXD-A21	A	RBD	IGHV1-24	IGHD6-13	IGHJ6	TTDRLGQQLAKGYYYYGMDV	20	2.7	IGLV3-1	IGLJ2	QAWDRTTPV	9	2.8
KXD-A22	A	NTD	IGHV4-59	IGHD2-15	IGHJ6	ARGGYDYYGMDV	12	5.9	IGLV1-40	IGLJ2	QSFDNSLSVHVL	12	3.4
KXD-A23	A	RBD	IGHV3-15	IGHD3-22	IGHJ4	KTEFGTYYYDTNGYDY	16	3.0	IGLV3-1	IGLJ2	LAWDRSTGV	9	3.6
KXD-A24	A	NTD	IGHV4-39	IGHD6-13	IGHJ4	ARQRVGSSWYYSDS	14	6.4	IGLV1-44	IGLJ1	AAWDDSLNGSYV	12	2.0
KXD-A25	A	RBD	IGHV3-43	IGHD2-15	IGHJ4	ATSEVDYFEY	10	3.8	IGKV4-1	IGKJ2	QQYYSTPPYT	10	3.0
KXD-A31	A	NTD	IGHV4-39	IGHD2-15	IGHJ4	ARDSPLGFCSASSCYFVDS	19	3.3	IGLV1-36	IGLJ1	AAWDDSLNGFV	11	3.4
KXD-A33	A	NTD	IGHV4-38	IGHD2-15	IGHJ5	ARQDAGSTQFDL	12	6.1	IGLV1-40	IGLJ3	QSYDGSLSGWV	11	2.3
KXD-A34	A	NTD	IGHV3-49	IGHD3-9	IGHJ6	TREDPRYNFDWLPSGMDV	18	4.0	IGKV1-39	IGKJ2	QQSYSTLYT	9	2.9
KXD-A43	A	NTD	IGHV4-39	IGHD5-12	IGHJ4	ARLREWDIVAGGGVFDY	17	6.1	IGLV3-1	IGLJ3	QSWDSSTAV	9	2.9
KXD-A48	A	NTD	IGHV4-39	IGHD2-15	IGHJ4	TRDSPLGHCGGSSCYYVGY	19	6.4	IGLV1-36	IGLJ1	AAWDDSLNGYV	11	3.1
KXD-A49	A	RBD	IGHV1-18	IGHD3-3	IGHJ4	ARDRGFWSGFDS	12	3.1	IGLV6-57	IGLJ2	QSYDSGIVV	9	2.8
KXD-A5	A	NTD	IGHV1-18	IGHD1-26	IGHJ4	ARVGESSGYSRSWRNEFDY	19	5.5	IGKV2-40	IGKJ1	MQRLDSPWT	9	4.6
KXD-A51	A	NTD	IGHV2-5	IGHD3-22	IGHJ4	ARSSPEIYYYDSSDYYQYYFDY	22	5.6	IGLV1-47	IGLJ1	AAWDDSLSGPYV	12	1.0
KXD-A52	A	NTD	IGHV3-49	IGHD3-9	IGHJ6	TRGDPRYNFDWLPDGMDV	18	2.3	IGKV1-39	IGKJ2	QQSYSTLYT	9	2.5
KXD-A56	A	NTD	IGHV3-49	IGHD3-9	IGHJ6	SREDPRYNFDWVPDGMDV	18	6.3	IGKV1-39	IGKJ2	QQSYSTLYT	9	7.5
KXD-A57	A	NTD	IGHV4-38	IGHD2-15	IGHJ5	ARQDAGSTQFDP	12	7.4	IGLV1-40	IGLJ3	QSYDGRLSGWV	11	3.1
KXD-A60	A	NTD	IGHV4-39	IGHD5-12	IGHJ4	ARLREWDIVAGGGVFDY	17	6.0	IGLV3-1	IGLJ3	QSWDSSTAV	9	1.8
KXD-A63	A	NTD	IGHV4-39	IGHD6-13	IGHJ4	ARERVGSSWYYSDY	14	1.3	IGLV1-44	IGLJ1	AAWDDGLNGSNV	12	0.7
KXD-A67	A	NTD	IGHV4-39	IGHD2-15	IGHJ4	TRDSPLGYCSGSSCYFVDY	19	5.4	IGLV1-36	IGLJ1	ATWDDSLNGYV	11	2.4
KXD-A69	A	RBD	IGHV1-24	IGHD5-24	IGHJ6	TTNGLQQKAVGVYYYYYYGLDV	21	4.7	IGLV3-1	IGLJ2	QAWDSSTAV	9	2.2
KXD-A70	A	NTD	IGHV4-39	IGHD3-10	IGHJ5	ARMVQPENWFDP	12	7.4	IGLV1-36	IGLJ2	AAWDHSLNGVI	11	2.7
KXD-A77	A	NTD	IGHV1-18	IGHD6-13	IGHJ4	ARVGESSGYSRSWRNEIDY	19	5.8	IGKV2-40	IGKJ1	MQRIEFPWT	9	2.6
KXD-A78	A	NTD	IGHV4-39	IGHD2-15	IGHJ4	TRDSPLGFCRGGSCYFVDY	19	3.4	IGLV1-36	IGLJ1	AAWDDSLNAYV	11	1.7
KXD-A8	A	RBD	IGHV3-74	IGHD3-22	IGHJ6	ARFSGLSGGYYYGMDV	16	2.7	IGLV6-57	IGLJ2	QSYDNSDLV	9	4.2
KXD-A82	A	NTD	IGHV4-39	IGHD2-15	IGHJ4	ARDSPLGSCSDSSCYFVDS	19	8.2	IGLV1-36	IGLJ1	AAWDDNLNGFV	11	2.4
KXD-A84	A	NTD	IGHV4-59	IGHD2-15	IGHJ6	ARGGYDYYGMDV	12	3.8	IGLV1-40	IGLJ2	QSYDDSLSVHVV	12	3.1
KXD-B6	B	RBD	IGHV3-30	IGHD2-2	IGHJ6	AGEGEDGFCSSLSCYSSPGGV	21	8.1	IGKV2-30	IGKJ4	MQGTHWPPLT	10	3.6
KXD-C10	C	NTD	IGHV4-39	IGHD3-9	IGHJ4	ARVVYYDILTGQKTFDY	17	5.1	IGLV1-51	IGLJ3	GTWDSSLSAGV	11	3.0
KXD-C12	C	NTD	IGHV4-39	N/A	IGHJ5	ARQLPTENWFDP	12	7.0	IGLV3-21	IGLJ2	QVWDNRSHHLVS	12	3.9
KXD-C14	C	NTD	IGHV3-33	IGHD3-3	IGHJ4	ARDSSYYDLWSGLDY	15	5.4	IGKV1-16	IGKJ2	QQYYSFPYT	9	5.3
KXD-C15	C	RBD	IGHV5-51	IGHD5-18	IGHJ4	ARPTSTDTASDY	12	5.1	IGKV1-39	IGKJ1	QQSYSPLWT	9	2.6
KXD-C18	C	RBD	IGHV3-33	IGHD1-26	IGHJ6	ARESEDSGGPGI	12	6.1	IGKV2-28	IGKJ2	MQALQTPRCT	10	1.3
KXD-C19	C	NTD	IGHV3-7	IGHD2-15	IGHJ6	ARERFCSAGSCYSFLGRRVYYYDGMDV	27	2.7	IGKV1-39	IGKJ1	QQSYSIPPT	9	4.7
KXD-C21	C	RBD	IGHV3-21	N/A	IGHJ3	ARGHAEEGDAFDT	13	5.8	IGKV1-5	IGKJ1	QQYNGFPWT	9	3.6
KXD-C23	C	RBD	IGHV3-48	IGHD6-13	IGHJ5	ARDPVCGYSSSCPLFGS	17	4.7	IGLV1-40	IGLJ3	QSYDSSLSGNWV	12	4.7
KXD-C24	C	RBD	IGHV5-51	IGHD3-9	IGHJ4	ARLPSVGHFDWGYFDY	16	6.0	IGKV3-20	IGKJ1	QQYGGSPPWT	10	5.2
KXD-C25	C	NTD	IGHV4-30	IGHD3-3	IGHJ5	ARTIFGDPNDWFDP	14	5.4	IGLV1-40	IGLJ2	QSYDTSLNGWDVV	13	2.0
KXD-C26	C	NTD	IGHV4-39	IGHD6-13	IGHJ4	ARHDFDIATADTSFHY	16	3.7	IGLV3-1	IGLJ3	QTWDNSAVV	9	6.9
KXD-C27	C	NTD	IGHV4-39	N/A	IGHJ5	ARQTPPNCFDP	11	2.0	IGLV3-21	IGLJ3	QVWDNGNDHPGV	12	3.2
KXD-C28	C	RBD	IGHV3-66	IGHD2-21	IGHJ5	ARGPFRKFDP	10	6.9	IGKV1-33	IGKJ2	QQYDNIPYT	9	3.9
KXD-C29	C	NTD	IGHV4-39	IGHD2-2	IGHJ4	ARHDFDIVTANTIFHY	16	5.1	IGLV3-1	IGLJ2	QTWDSSAVV	9	4.6
KXD-C31	C	NTD	IGHV4-39	IGHD7-27	IGHJ6	ARSGDSLFYYYYYYMDV	17	5.7	IGKV4-1	IGKJ4	QQYYSVPLT	9	4.4
KXD-C36	C	NTD	IGHV4-39	IGHD3-9	IGHJ5	ARHVDYDIVTDSGRFDP	17	10.0	IGLV3-1	IGLJ3	QTWDSGSGV	9	3.6
KXD-C4	C	RBD	IGHV3-30	IGHD5-18	IGHJ4	AREHESETAVDK	12	5.1	IGKV1-12	IGKJ4	QQANNFHLT	9	5.3
KXD-C40	C	NTD	IGHV4-39	IGHD2-2	IGHJ4	ARHDFDIVTANTIFHY	16	6.4	IGLV3-1	IGLJ2	QTWDSSAVV	9	4.9
KXD-C44	C	RBD	IGHV3-11	IGHD6-13	IGHJ1	ASLGYSTIWDGSAEYFQH	18	2.7	IGKV1-39	IGKJ4	QQSYSTPRT	9	0.7
KXD-D3	D	RBD	IGHV4-4	IGHD1-14	IGHJ6	ARDGPHTTSPQDDYYYMDV	19	6.4	IGKV2-29	IGKJ5	MQGRLSPRT	9	5.3
KXD-E1	E	RBD	IGHV3-53	IGHD5-18	IGHJ4	ARLGGYGRKDYDH	13	7.2	IGKV1-33	IGKJ2	HQYDNVPPT	9	5.6
KXD-E2	E	RBD	IGHV1-69	IGHD2-2	IGHJ3	AHTPLPSPCHADALDI	16	13.1	IGKV1-39	IGKJ3	QQSHGSPFT	9	9.2
KXD-E3	E	RBD	IGHV1-69	IGHD4-17	IGHJ3	ARERVDYGDRLLNGSAFDI	19	9.8	IGKV3-20	IGKJ3	QLCGGSAPT	9	6.2
KXD-E4	E	RBD	IGHV3-53	IGHD1-26	IGHJ4	VKMEWDLL	8	6.9	IGKV1-5	IGKJ1	QQYIVYPWT	9	6.1
KXD-F1	F	RBD	IGHV4-34	IGHD3-10	IGHJ4	ARGYRDYGRGMFPLGN	16	11.3	IGKV3-11	IGKJ1	QQRDNWPPT	9	5.0
KXD-F10	F	RBD	IGHV4-30	IGHD3-9	IGHJ6	ARANLLTFHVDV	12	8.4	IGLV6-57	IGLJ2	QSYDGSKVV	9	3.2
KXD-F12	F	RBD	IGHV4-30	IGHD5-12	IGHJ5	ARLRLLVNWFDP	12	4.0	IGLV6-57	IGLJ3	QSYDGSNVV	9	2.1
KXD-F3	F	RBD	IGHV3-9	IGHD1-1	IGHJ4	AKDFHNNWYPGRFDF	15	2.0	IGKV1-33	IGKJ5	QQYDNVPL	8	3.8
KXD-F6	F	RBD	IGHV3-33	IGHD2-2	IGHJ6	AKDMAYYLLVPEARPPYGMDV	21	2.7	IGKV3-20	IGKJ3	HQYGGSPFT	9	4.3
KXD-G10	G	RBD	IGHV4-30	IGHD7-27	IGHJ4	ARALGIIDY	9	8.1	IGKV1-NL1	IGKJ5	QQYYSTPT	8	4.9
KXD-G23	G	RBD	IGHV4-4	IGHD3-10	IGHJ4	ARARGIIDY	9	10.5	IGKV1-NL1	IGKJ4	QQYYSTPS	8	5.1
KXD-G26	G	RBD	IGHV1-69	IGHD2-2	IGHJ4	ATNAPYCTSTACFNF	15	10.3	IGLV1-40	IGLJ2	QSYDSGLSASV	11	7.7
KXD-G32	G	NTD	IGHV4-39	IGHD1-26	IGHJ5	ARLAWDFALSFHWFDP	16	12.5	IGLV2-11	IGLJ2	CSYGGADSWV	10	3.3
KXD-G33	G	RBD	IGHV1-24	IGHD3-16	IGHJ4	AAGGLHMSLGIMPFDY	16	8.5	IGLV1-47	IGLJ3	ASWDDSLSGRGQGV	14	7.8
KXD-G44	G	NTD	IGHV4-39	IGHD3-3	IGHJ4	ARHPAHDFWSGYFDN	15	7.1	IGKV3-15	IGKJ5	QQYNEWPRFS	10	2.9
KXD-G5	G	RBD	IGHV4-39	IGHD7-27	IGHJ4	ARTLGMFDH	9	8.1	IGKV1-NL1	IGKJ3	QQYYDTPFT	9	5.8
KXD-G6	G	RBD	IGHV4-4	IGHD6-13	IGHJ4	TSVLGTFDY	9	12.2	IGKV1-NL1	IGKJ5	QQYYTTRT	8	6.0
KXD-I29	I	RBD	IGHV3-9	IGHD3-10	IGHJ5	TKGQVGELPFPLDS	14	8.5	IGLV1-44	IGLJ2	AAWDDTLNSLV	11	4.7
KXD-I39	I	NTD	IGHV3-15	IGHD3-9	IGHJ4	NTERDNLNFGDY	12	5.6	IGKV1-33	IGKJ2	QQYANLPRT	9	5.6
KXD-I42	I	RBD	IGHV3-9	IGHD3-10	IGHJ4	AKGQLGEFPFPVDF	14	5.8	IGLV1-44	IGLJ3	AVWDDRVNGLV	11	7.1
KXD-J16	J	RBD	IGHV1-46	IGHD4-11	IGHJ5	ARGVYSNYEDWFDP	14	3.4	IGKV4-1	IGKJ5	QQYYTSPLT	9	1.3
KXD-J21	J	RBD	IGHV1-46	IGHD4-11	IGHJ5	ARGVYSNYEDWFDP	14	3.1	IGKV4-1	IGKJ4	QQYYTTPLT	9	3.0
KXD-J23	J	RBD	IGHV3-33	IGHD3-3	IGHJ2	AREGYDFWGDSPENWYFDF	19	4.7	IGLV2-11	IGLJ1	CSYTGTYTYV	10	3.8
KXD-J28	J	RBD	IGHV1-18	IGHD2-2	IGHJ6	GRVESHIVLVPSAGPYYYYMDV	22	11.6	IGLV1-44	IGLJ1	AAWDDSLNSYV	11	8.1
KXD-J33	J	NTD	IGHV3-33	IGHD4-17	IGHJ4	ARDFYWSQADDYGDPHWPGG	20	4.1	IGLV3-10	IGLJ2	YSADGTAYHRGV	12	4.8
KXD-J37	J	RBD	IGHV3-53	IGHD3-16	IGHJ4	TRVLPGGQYFDY	12	9.9	IGKV3-20	IGKJ2	QQYESPAMYI	10	4.0
KXD-J39	J	RBD	IGHV3-33	IGHD3-3	IGHJ2	AKEGYDFWGADPENWYFDL	19	0.7	IGLV2-11	IGLJ1	CSYAGPYTYV	10	4.7
KXD-J42	J	RBD	IGHV1-18	IGHD2-2	IGHJ6	ARVDSHIVLVTAAIPDYYYMDV	22	9.5	IGLV1-44	IGLJ1	AAWDVSLNGYV	11	8.8
KXD-J44	J	RBD	IGHV1-18	IGHD2-21	IGHJ6	ARVNSHIVMVASATPYYYYMDV	22	11.3	IGLV1-44	IGLJ1	AAWDASLNAYV	11	7.5
KXD-J47	J	RBD	IGHV1-18	IGHD2-21	IGHJ6	ARVDSHIVAVPAAIPDYFYMDV	22	11.5	IGLV1-44	IGLJ1	AGWVHTLNGYV	11	11.2
KXD-J5	J	RBD	IGHV1-18	IGHD2-21	IGHJ6	ARVDSHIVMVASAIPYYYHLDA	22	9.9	IGLV1-44	IGLJ1	AAWDASLNAYV	11	7.9
KXD-J6	J	RBD	IGHV1-18	IGHD2-2	IGHJ6	ARVDSHIVSVPSAIPFYYYMDV	22	9.6	IGLV1-44	IGLJ1	AAWDASLNAYV	11	3.4
KXD-J8	J	RBD	IGHV3-33	IGHD3-3	IGHJ2	AKEGYDFWGADPEDWYFDL	19	2.4	IGLV2-11	IGLJ1	CSYAGPYTYV	10	4.2
KXD-K19	K	RBD	IGHV3-66	IGHD3-16	IGHJ4	ARDLLEAGGTDY	12	6.5	IGKV3-20	IGKJ3	QFYSTIAVT	9	5.9
KXD-K20	K	RBD	IGHV3-9	IGHD3-22	IGHJ4	AKAGDASGYYSDFVY	15	5.1	IGLV2-11	IGLJ2	CSFAGGYTWV	10	2.7
KXD-K29	K	NTD	IGHV4-39	IGHD2-21	IGHJ4	ARLSVGTASTYFDY	14	6.1	IGLV1-44	IGLJ3	AAWDDSLNGHWV	12	2.0
KXD-K3	K	RBD	IGHV3-66	IGHD3-22	IGHJ4	TRDLGGYYDQ	10	9.9	IGKV1-5	IGKJ1	QQYNTDSRT	9	3.9
KXD-K40	K	RBD	IGHV3-66	IGHD3-22	IGHJ4	ARDLGGYFDH	10	8.9	IGKV1-5	IGKJ1	QQYSTDSRT	9	5.6
KXD-K48	K	NTD	IGHV4-39	IGHD5-12	IGHJ5	ARHVWDIALRKDWFDP	16	7.1	IGKV3-20	IGKJ1	QQYGSSRT	8	2.1